Band-theory approach to the study of local magnetization fluctuations in Fe and Ni



1991 J. Phys.: Condens. Matter 3 7663

(http://iopscience.iop.org/0953-8984/3/39/012)

J. Phys.: Condens. Matter 3 (1991) 7663–7682. Printed in the UK

# Band-theory approach to the study of local magnetization fluctuations in Fe and Ni

L M Sandratskii and E N Kuvaldin
Institute of Metal Physics, Sverdlovsk 620219, USSR

Received 7 November 1990, in final form 22 May 1991

**Abstract.** A calculation scheme is discussed that permits the investigation of both transverse and longitudinal fluctuations of local magnetization in 3d magnets. It is based on the use of a band-structure calculation method for the study of excited magnetic states. Calculations were carried out for body-centred cubic Fe and face-centred cubic Ni. The probability distribution of the local magnetic moment length is evaluated for the paramagnetic region. Some comparisons are made, illustrating the role of longitudinal fluctuations as well as the role of electronic characteristics of excited states.

## 1. Introduction

In spite of the success of band-structure calculations in the description of the ground-state properties of ferromagnetic 3d metals [1], the explanation of the temperature dependences of these properties on the basis of the traditional Stoner approach meets major difficulties [2]. At present it is commonly acknowledged that overcoming these difficulties is possible only within the framework of a theory combining the concept of the itinerant nature of electrons with allowance for local fluctuations of magnetization. A variety of such theoretical approaches have been suggested (see e.g. [2–7]), which differ substantially in the models of electronic interactions adopted.

Most of the research (let us call it approach I) was carried out with the use of a phenomenological expression for the free energy of the problem or within the framework of the one-band Hubbard model [2, 4, 7]. This allows one to estimate electronic characteristics of the excited states of a magnetic crystal without using quite complicated and time-consuming methods of electronic energy structure calculations. These calculations have permitted a qualitative or semi-quantitative description of numerous experiments to be made. However, the quantitative reliability of these methods is restricted.

Therefore, there is strong interest in the development of approaches based on more complicated models of interactions defining the electronic structure. These models demand the use of band-structure calculation methods. Along this line there is also plenty of work, which, in turn, can be subdivided into two subgroups. The first subgroup (approach IIa) contains calculations carried out with the KKR-CPA (Korringa–Kohn–Rostoker coherent-potential approximation) method (see [5, 8, 9] and further papers). The theoretical scheme suggested here [5] is a substantial step in the extension of the density-functional theory to problems concerning the thermodynamics of itinerant

0953-8984/91/397663 + 20 $03.50 

magnets. Unfortunately, this scheme is so complicated that, despite the use of the single-site approximation, concrete calculations have been carried out for the paramagnetic state only.

Unlike the KKR-CPA method, which is aimed at a direct calculation of statistically averaged values, the second subgroup of investigations (approach IIb) puts an accent on the detailed study of electronic characteristics of individual excited non-collinear magnetic configurations [6]. On the basis of these calculations, estimations of various physical parameters were made [10, 11] and conclusions on the tendencies in the temperature behaviour of physical properties were drawn [10–17]. The results of the calculations of separate magnetic structures were used for simple parametrizations of the complete variety of excited magnetic configurations and, in the next step, for the construction of various schemes of statistical averaging [11, 14, 18].

On the whole, each of the approaches—I, IIa and IIb—has its own advantages. Therefore, these approaches are to be considered as supplementary to one another. However, besides the differences connected with the adopted model of electronic interactions, there is another important difference that concerns the allowance for the longitudinal fluctuations of local magnetization, which may lead to difficulties in comparing the results of different approaches.

In most papers belonging to approach I the longitudinal fluctuations of local magnetization are taken into account. These fluctuations are introduced into the theory either phenomenologically or, more consistently, using the Stratonovich–Hubbard transformation for the Hubbard Hamiltonian partition sum. In the first case the free energy $F$ of a system is estimated by the formula [2]

$$\exp(-F/T) = \int \delta m(r) \exp\{-\Psi[m(r)]/T\} \tag{1}$$

where the functional integral is carried out over various spin densities, which are treated classically. Here it is supposed that each spin configuration corresponds to a crystal excited state considered in adiabatic approximation; $\Psi[m(r)]$ is the energy functional. In the second case, using the Stratonovich–Hubbard transformation and static approximation [2, 4, 7], each excited state is connected with a definite configuration of atomic 'exchange' fields, which assume arbitrary values and directions. The fluctuations of values and directions of exchange fields are closely connected with the fluctuations of the corresponding characteristics of the atomic magnetic moments.

On the other hand, in approaches IIa and IIb the amplitude fluctuations of magnetic moments were not considered. Each excited state was defined by the directions of atomic moments, the lengths of which are to be found in self-consistent calculations. Thus, from all configurations with given directions of magnetic moments, only the one with the lowest energy is considered.

This difference between approaches I and II is very important and may substantially influence the estimation of such significant physical parameters as the average value of the local atomic moment and its longitudinal stiffness [2]. Moreover, the correctness of the notation of well defined local moment may be substantially dependent on the magnitude and character of such fluctuations. The longitudinal fluctuations of magnetic moments can noticeably influence the peculiarities of a magnetic phase transition [2, 19].

In the present paper we make an attempt to study the longitudinal fluctuations of atomic moments within the framework of approach IIb. In section 2, we discuss a computational scheme allowing one to use band-structure calculation methods for the investigation of longitudinal fluctuations. In section 3, the results of studying peculiarities

of static longitudinal fluctuations in Fe and Ni are given. In section 4, a simple statistical averaging is carried out to obtain an estimation of the local magnetic moment length distribution. This distribution is compared with the counterpart calculated within approach I. The temperature dependence of the average local magnetic moment in the paramagnetic state is also estimated.

## 2. Calculation technique

As follows from the introduction, one of the main purposes of the present work is the study, by means of band-theory methods, of total energy $E(\{m_n\})$ as a function of lengths and directions of magnetic moments of all atoms. Evidently, the exact calculation of $E(\{m_n\})$ is not possible and one must use some, simple, parametrization of this dependence [14, 18]. Previous calculations of non-collinear magnetic configurations of iron [11, 13, 14] have shown that the average angle between magnetic moments of nearest neighbours is an important parameter characterizing electronic structure. If we take into consideration longitudinal fluctuations of local moments, it is necessary to introduce also a parameter characterizing the average length of moments. We shall suppose that local electronic characteristics of a given atom are defined by two parameters: an average angle between magnetic moments of the given and neighbouring atoms, and an average length of these atoms' magnetic moments. The easiest way to estimate these parametric dependences is the calculation of the electronic characteristics of spiral magnetic configurations. Previous investigations [6, 10–15] have shown that the study of a sufficiently wide set of the simplest non-collinear configurations—spiral configurations—allows one to draw important conclusions concerning the temperature behaviour of 3d magnets.

The method used for the calculation of spiral structures is described in section 2.1. Peculiarities of the calcuation of excited states are discussed in section 2.2.

### *2.1. Method of band-structure calculations for spiral magnetic configurations*

Generalizations of various methods of band-structure calculations in the case of non-collinear magnetic configurations were suggested in [6, 20–24]. A substantial part of the calculations of non-collinear configurations was devoted to spiral magnetic structures. In [6, 10–12] a large cluster was considered. The calculations were carried out for the tight-binding Hamiltonian with the recursion method. In [21, 22] it was shown that allowance for the generalized symmetry of the problem permits one to simplify the calculation fundamentally. This property was used in [14, 15], where the calculations were carried out by the KKR method.

A comparison of the results obtained with the KKR method [14] and those obtained on the basis of the tight-binding Hamiltonian [6, 10, 11] shows that they are close enough if the tight-binding scheme includes s, p and d electron states. As the use of the KKR method needs much more computer time, in the present work all calculations were carried out with the tight-binding method (TBM).

Let us write the one-electron Hamiltonian of a non-collinear magnetic configuration in the form

$$H = -\Delta + \sum_n U^n V(|r - t_n|)(U^n)^{-1} \tag{2}$$

where

$$V(r) = [V_C(r) + V_{ex}(r)]I + \Delta V_{ex}(r) \tag{3}$$

$$\Delta V_{ex}(r) = \begin{pmatrix} -\Delta V_{ex}(r) & 0 \\ 0 & \Delta V_{ex}(r) \end{pmatrix}. \tag{4}$$

In (2)–(4), $V_C$ is the atomic Coulomb potential; $V_{ex} \pm \Delta V_{ex}$ are the components of the exchange potential that act on electronic states with correspondingly negative and positive spin projection on the atomic moment direction; $I$ is the unit matrix of second order; $t_n$ are the lattice vectors; and $U^n$ is the matrix of spin rotation [22] connecting the global coordinate system with the local coordinate system, the $z$ axis of which is parallel to the magnetic moment of the $n$th atom.

In the present paper we consider spiral magnetic configurations

$$e_n = (\sin\beta\cos(q \cdot t_n), \sin\beta\sin(q \cdot t_n), \cos\beta) \tag{5}$$

where $e_n$ is a unit vector parallel to the $n$th atom magnetic moment, $q$ is the vector of spiral, and $\beta$ is the angle between the $z$ axis of the global coordinate system and atomic moments.

The basis functions for the expansion of the crystal electronic state $\Psi(r)$ are constructed from the one-centre functions, which have the form $\varphi_{\gamma\sigma}(r)\chi_\sigma$ in the local coordinate systems. Here $\gamma$ labels different atomic-like functions with given $\sigma$, and

$$\chi_+ = \begin{pmatrix} 1 \\ 0 \end{pmatrix} \qquad \chi_- = \begin{pmatrix} 0 \\ 1 \end{pmatrix}.$$

Taking into consideration the generalized Bloch theorem [22] we shall use basis functions

$$\Phi_{\gamma\sigma k}(r) = N^{-1/2} \sum_n \exp(ik \cdot t_n)\, \varphi_{\gamma\sigma}(|r - t_n|)U^n\chi_\sigma \tag{6}$$

and the decomposition takes the form

$$\Psi_k(r) = \sum_{\gamma\sigma} C_{\gamma\sigma k}\Phi_{\gamma\sigma k}(r). \tag{7}$$

Supposing that functions (6) are orthonormal we obtain the following system of linear equations:

$$\sum_{\gamma\sigma} (T_{\gamma\sigma,\gamma'\sigma'} + V_{\gamma\sigma,\gamma'\sigma'} - \delta_{\gamma\sigma,\gamma'\sigma'}E)C_{\gamma\sigma} = 0. \tag{8}$$

(We omit the index showing the dependence of quantities on $k$.) Here

$$T_{\gamma\sigma,\gamma'\sigma'} = \sum_n \exp(ik \cdot t_n)\chi_\sigma^+ (U^0)^{-1}U^n\chi_{\sigma'} \int \varphi_{\gamma\sigma}^*(r)(-\Delta)\varphi_{\gamma'\sigma'}(r - t_n)\,dr \tag{9}$$

$$V_{\gamma\sigma,\gamma'\sigma'} = \sum_{nn'} \exp[-ik \cdot (t_n - t_{n'})]\chi_\sigma^+ (U^n)^{-1}U^0 \times \left(\int \varphi_{\gamma\sigma}^*(r - t_n)V(r)\varphi_{\gamma'\sigma'}(r - t_{n'})\,dr\right)(U^0)^{-1}U^{n'}\chi_{\sigma'}. \tag{10}$$

If we suppose that in formula (10) only the one-centre (i.e. $n = n' = 0$) integrals of the potential (3) are not equal to zero, then the secular matrix of the problem (8) may be represented in the form

$$\begin{pmatrix} \cos^2(\frac{1}{2}\beta)H_+(\boldsymbol{k}-\frac{1}{2}\boldsymbol{q})+\sin^2(\frac{1}{2}\beta)H_+(\boldsymbol{k}+\frac{1}{2}\boldsymbol{q}) & -\frac{1}{2}\sin\beta[H_0(\boldsymbol{k}-\frac{1}{2}\boldsymbol{q})-H_0(\boldsymbol{k}+\frac{1}{2}\boldsymbol{q})] \\ -\frac{1}{2}\sin\beta[H_0(\boldsymbol{k}-\frac{1}{2}\boldsymbol{q})-H_0(\boldsymbol{k}+\frac{1}{2}\boldsymbol{q})] & \sin^2(\frac{1}{2}\beta)H_-(\boldsymbol{k}-\frac{1}{2}\boldsymbol{q})+\cos^2(\frac{1}{2}\beta)H_-(\boldsymbol{k}+\frac{1}{2}\boldsymbol{q}) \end{pmatrix}. \tag{11}$$

Here, $H_\sigma(\boldsymbol{k})$ is the secular matrix of the traditional TBM written for ferromagnetic crystal states with spin projection $\sigma$, which experience the potential $V_C + V_{ex} - \sigma\Delta V_{ex}$; $H_0(\boldsymbol{k})$ is the secular matrix of the TBM corresponding to the non-magnetic crystal with $\Delta V_{ex} = 0$.

The form (11) of the secular matrix is convenient for calculations because it reduces the construction of the spiral-structure matrix mainly to the calculation of the secular matrix of the traditional TBM. Formula (11) is exact for the Hamiltonian used in [6, 10, 11] due to neglect of multicentre integrals of the exchange potential.

In the present work we also use formula (11). The calculation of matrices $H_\sigma$ and $H_0$ was carried out on the basis of the interpolation scheme of Slater and Koster [25]. Parameters of the scheme were constructed on the basis of parameters from [26].

In our calculations the value of the atomic magnetic moment may deviate from its value in the ferromagnetic ground state [26] as a result of both non-collinearity of atomic spins and allowance for longitudinal fluctuations of magnetic moment. To take this property into consideration, we used the following supposition. Let $C^0_\sigma$ be the interpolation scheme parameters of [26], which correspond to the ferromagnetic states with spin projection $\sigma$ ($\sigma = \pm 1$) on the magnetization direction. If, in the next step of the iteration process, an initial atomic moment was equal to $m_{in}$, then the matrix $H_\sigma$ in (11) was calculated with the use of the parameters

$$C_\sigma = \tfrac{1}{2}(C^0_+ + C^0_-) + \tfrac{1}{2}\sigma(C^0_+ - C^0_-)m_{in}/m_0(0) \tag{12}$$

where $m_0(0)$ is the atomic moment of the ferromagnetic ground state. To calculate $H_0$ we used parameters (12) corresponding to $m_{in} = 0$.

It is necessary to note that, when the formula (12) is used for all coefficients of the interpolation scheme, the form (11) of the secular matrix is not exact because in the derivation of (11) the spin dependence of one-centre contributions only was supposed. Nevertheless, in calculating diagonal blocks, we did not average coefficients $C_\sigma$ corresponding to multicentre contributions [26] because, first, the spin dependence of initial multicentre coefficients $C_\sigma$ is much less than the $\sigma$ dependence of corresponding one-centre coefficients, and secondly, formula (11) is exact for the limiting cases of ferromagnetic and non-magnetic crystals, which allowed us to obtain in the ferromagnetic case the results of [26].

As we have assumed a dependence of coefficients (12), and therefore of secular matrix (11), on the atomic moment value, this value is to be calculated self-consistently. Using the results of band calculations the projection of the $n$th atom magnetic moment on the direction $\boldsymbol{e}_n$ defined by (5) may be found from the formula

$$m_{out} = \sum_{\sigma\gamma k} C_{\gamma\sigma k} \tag{13}$$

where the summation is carried out over filled states. For each magnetic configuration, the self-consistency condition may be written in the form $m_{out} = m_{in}$.

To calculate the parametric dependence of total energy we have chosen spiral structures demanding the lowest computation time. In the case of BCC Fe, the spiral structures with $\boldsymbol{q} = (0, 0, 2\pi/a)$ and various $\beta$ (those are the structures called 'alternating tilt' in [6, 10, 11]) were chosen for calculations because for these magnetic configurations the volume of the reciprocal-space irreducible domain (ID) is equal to the 1/48th Brillouin zone (BZ) volume [27]. If we denote by $\theta$ an average angle between the spin of the given atom and the spins of neighbouring atoms, for this type of spiral structure $\theta = 2\beta$.

Symmetry analysis [27] shows that in the case of FCC Ni, the minimal volume of the ID is equal to the 1/16th BZ volume. In particular, this volume of the ID is realized for the spiral structures with $\boldsymbol{q} = (0, 0, 2\pi/a)$ and arbitrary $\beta$ (for such spiral structures $\theta = \frac{4}{3}\beta$) and also for plane spiral structures with $\beta = 90°$ and any $q$ parallel to the $z$ axis (here $\theta = qa/3$). We carried out calculations of electronic characteristics of both spiral structures.

### 2.2. *Calculation of excited magnetic states*

As was noted above, our aim is the calculation of electronic characteristics for non-collinear magnetic configurations with given directions and lengths of atomic magnetic moments. In the traditional self-consistent band-structure calculation, these quantities cannot be evaluated because the complete self-consistency of lengths and directions of magnetic moments leads to the lowest energy state. In the cases of Fe and Ni this is the ferromagnetic ground state [1]. Therefore the calculation must be carried out with allowance for the restrictions imposed on the lengths and directions of atomic moments. In [5, 28–31] it is shown that the calculation with a constraint imposed on the parameters of magnetic moments is equivalent to self-consistent band-structure calculations free from these restrictions if each atom experiences the action of an 'exchange' or 'magnetic' field $\boldsymbol{h}_n$. (Note that here we can draw an analogy with the random 'exchange' fields appearing after the Stratonovich–Hubbard transformation of Hubbard Hamiltonian partition sum [2, 4, 7].)

At present there is a quite restricted number of band-structure calculations carried out for excited magnetic configurations. Investigations of excited magnetic states with collinear magnetic structure were carried out in [32–34] using the fixed-spin-moment method [28, 31]. For ferromagnetic configurations, calculations are simplified substantially owing to the fact that the electronic states of a ferromagnetic crystal are characterized by a definite value of the spin projection on the magnetization axis. This permits one not to change the traditional scheme of a ferromagnetic crystal calculation and to take the constraining fields into consideration only at the stage of the search for the order of filling of the electronic states [28, 31].

Non-collinear excited magnetic states were investigated within the framework of approaches IIa and IIb. As was mentioned in the introduction, longitudinal fluctuations of magnetic moments were not included in the considerations.

In [6, 10–17] belonging to approach IIb the projections of atomic magnetic moments on chosen directions were calculated self-consistently using a scheme analogous to that described in section 2.1. The magnetic moment components perpendicular to the chosen directions were not considered. This approach corresponds to the supposition that there exist fields $\boldsymbol{h}_n$ [28] perpendicular to the directions $\boldsymbol{e}_n$ and that the effect of these fields reduces to the suppression of the perpendicular component of magnetic moments.

Under the derivation of the formulae of the KKR-CPA method [5] used in approach

IIa there were also suppositions reducing the role of constraining fields to the suppression of magnetic density component perpendicular to vectors $e_n$. Therefore, as in approach IIa, the fields were not taken into consideration explicitly.

In the present paper we aim to investigate both the transverse and longitudinal spin fluctuations. Hence fields $h_n$ must, in general, have two non-zero components perpendicular and parallel to the corresponding vectors $e_n$. The most general form of the secular matrix used in our calculations may be written as

$$\begin{pmatrix} H_{++} - hE & H_{-+} + h_\perp E \\ H_{+-} + h_\perp E & H_{--} + hE \end{pmatrix} \tag{14}$$

where $H_{\sigma\sigma'}$ are the corresponding blocks of matrix (11), $h$ and $h_\perp$ are the parallel and perpendicular components of fields $h_n$ and $E$ is the unit matrix.

As non-collinear magnet states do not have definite spin indices, the influence of longitudinal component $h$ does not reduce merely to the shift in energy of the states calculated with $h = 0$. Therefore it is necessary to take the presence of the fields into consideration at the stage of energy spectrum calculations. The calculations were organized as follows. We fixed a value of $h$ and found the self-consistent values of $m$ corresponding to it.

We used two different schemes of self-consistent calculations. The first scheme (scheme A) is based on the supposition of [5, 6, 14] that the perpendicular component of the constraining field may be excluded from consideration if the magnetic moment component parallel to the chosen direction is calculated self-consistently but the perpendicular component is not taken into consideration. In the second scheme (scheme B) the perpendicular component $h_\perp$ of the field is taken into consideration explicitly. In the latter case it is necessary to find $h_\perp$ for which the perpendicular component of magnetic moment is equal to zero and simultaneously the longitudinal component is self-consistent. Note that, making an explicit allowance for $h_\perp$ (scheme B), one imposes conditions on both interdependent components of magnetic moments. Therefore the iteration procedure demands much more computational time.

Knowledge of the interconnection of magnetic moments $m_n$ and fields $h_n$ permits one to evaluate the total energy of excited states using the formula

$$\partial E(\{m_n\})/\partial m_n = h_n \tag{15}$$

obtained in [28] within the framework of the local density-functional theory (see also [29, 30, 32]).

Note that in recent work [35] dealing with a tight-binding Hamiltonian a formula was suggested for total energy which guarantees that total energy calculated numerically will be minimal for the self-consistent state, i.e. in the case of zero constraining fields. The method considered above satisfies this condition too.

## 3. Excited magnetic states of iron and nickel

### *3.1. Iron*

First let us consider the angular dependence of the self-consistent local magnetic moment calculated for zero longitudinal field $h$. We shall use the notation $m_0(\theta)$ for this function.

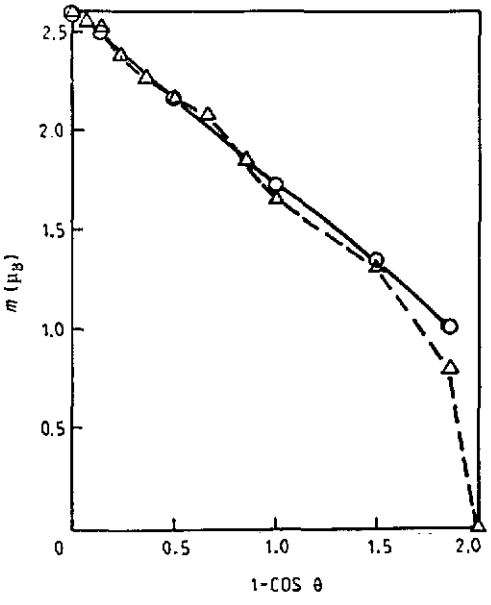


**Figure 1.** The $m_0(\theta)$ curves of Fe calculated using the physical model of [6]. Circles show our results; triangles represent the results of [6]. Our calculations have given also a zero branch of $m_0(\theta)$ lying within an angular interval from $\theta_b$ till 180°, where $\theta_b$ is less than 150°. (We did not aim to find the exact value of $\theta_b$.)

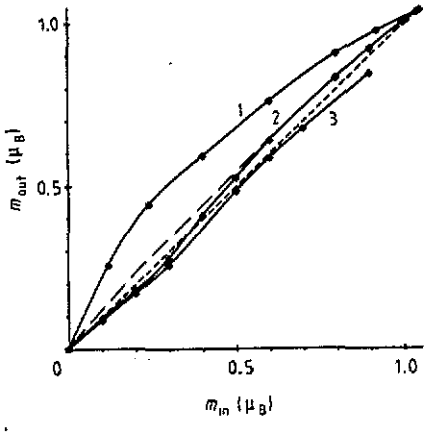


**Figure 2.** The $m_{out} = f(m_{in})$ curves of Fe calculated using the physical model of [6] for the values of angle $\theta$ equal to 0° (curve 1), 150° (curve 2) and 180° (curve 3). The broken straight line is the line $m_{out} = m_{in}$. The discussion of the broken curve attached to curve 2 is given in the text. For points of curve 1, both coordinates $m_{in}$ and $m_{out}$ are to be multiplied by 2.5

For iron, calculations of $m_0(\theta)$ have been carried out earlier in [6, 11, 14, 15]. It is useful to compare the results obtained with different models of Hamiltonian and various methods of calculation.

Figure 1 represents two curves $m_0(\theta)$, which were calculated with two different methods for the same physical model [6] making allowance for the d electrons only. On the whole, both calculations have given similar results. However there is a peculiarity that has not been noted in [6] but appeared in our calculations: the function $m_0(\theta)$ consists of two branches, each of which is defined only for a part of angle $\theta$ values. There is an angular interval where the calculation gives two different stable states of the system. To find all self-consistent solutions of the problem we restored the form of the curve $m_{out} = f(m_{in})$ for a wide range of $m_{in}$. Figure 2 shows the typical forms of calculated curves for three different intervals of angle $\theta$. Curve 1 corresponds to the case of one stable state of the system. The self-consistent moment of this state is not equal to zero. Curve 2 gives two stable states, one of which has zero magnetic moment. Finally, curve 3 corresponds to the case of large $\theta$, where the only self-consistent solution is equal to zero.

The form of angular dependence of $m_0$ obtained in our calculations (figure 1) is completely analogous to one of the curves discussed in [32, 33] in connection with the investigation of the volume dependence of the ferromagnetic atomic moment of 3d metals. Corresponding total energy curves versus atomic moment [32, 33] are shown

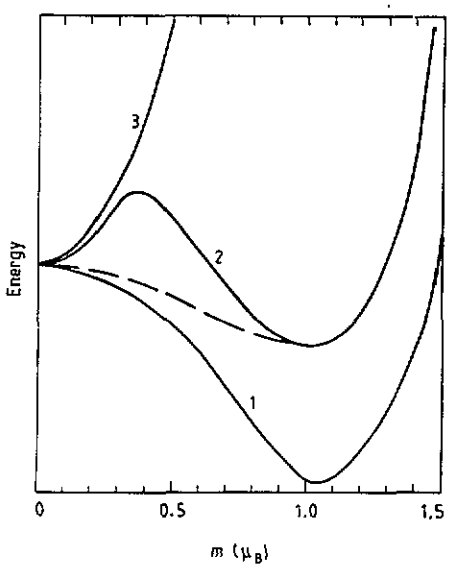


**Figure 3.** The schematic total energy curves corresponding to the curves $m_{out} = f(m_{in})$ shown in figure 2. For points of curve 1, coordinate $m$ is to be multiplied by 2.5.

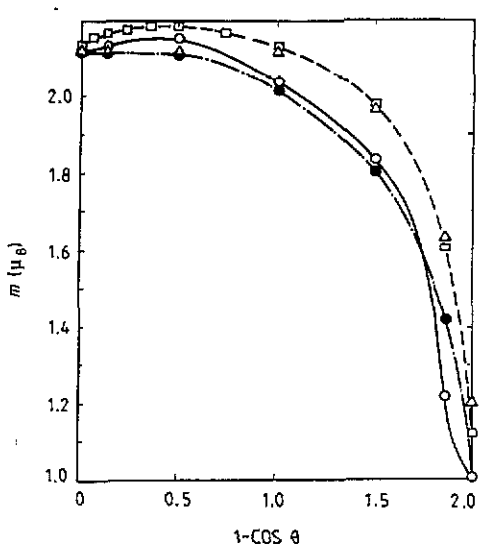


**Figure 4.** Angular dependence of $m_0$ for iron in various models: □, the results of [11]; △, the results of [14]; ●, the present calculation, scheme A; ○, the present calculation, scheme B. The present calculations have also given the zero branch of the function in the angular interval from $\theta_b$ till 180° (see figure 12).

schematically in figure 3. Curve 1 has the only minimum lying at non-zero moment value. Curve 2 has two minima and therefore gives two stable states of the system. With increase of $\theta$ the depth of the minimum at non-zero $m$ decreases and for a certain value of the angle this minimum disappears. Curve 3 gives the only minimum at $m = 0$. The maxima of the energy on curves 1 and 2 (figure 3) correspond to self-consistent values of $m$ also. But at these points the derivative of the function $m_{out} = f(m_{in})$ exceeds unity (figure 2). These states are unstable.

The form of the $m_0(\theta)$ curve, which assumes a continuous decrease of the magnetic moment from its maximal ferromagnetic value to zero in the antiferromagnetic limit [6], would correspond to the continuous transformation of the curve 1 minimum (figure 3) into the curve 3 minimum. In this case, the function $E(m)$ (figure 3) would have the only minimum for all of $\theta$, that is curves 2 in figures 2 and 3 should change in accordance with the broken curves shown in the figures.

Figure 4 compares the $m_0(\theta)$ curves calculated for various models of Hamiltonian, which take into consideration s, p and d electrons. There are important peculiarities common to all curves. First of all, there is a wide $\theta$ range where the value of the local magnetic moment is close to the ferromagnetic value. Then, the moment decreases rapidly to values close to 1 $\mu_B$. The peculiarities of the electronic structure of iron, which are responsible for such behaviour of the magnetic moment, were discussed in [14, 15].

Calculations for the model Hamiltonian discussed in section 2.1, like aforementioned calculations for the model of [6], give two branches of the $m_0(\theta)$ function. The second branch is defined for an angular interval from $\theta_b$ to 180° and assumes values equal to

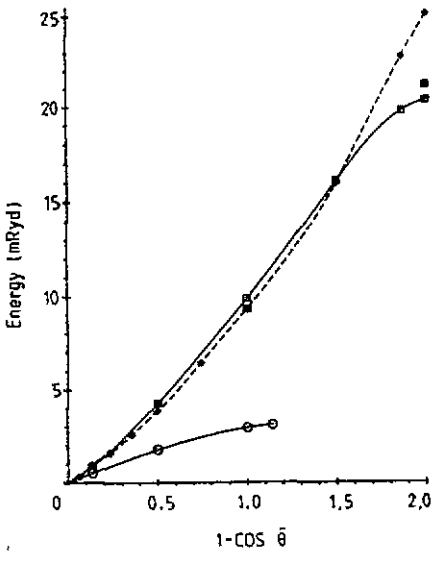


**Figure 5.** The $E_0(\theta)$ curves for iron and nickel. Iron: □, the results obtained with formula (16); ■, the points obtained with the use of formula (17); the broken curve represents the results of [11]. Nickel: ○, the results obtained with formula (16). All calculations were carried out for spiral structures with $q = (0, 0, 2\pi/a)$. Here we use the angle $\bar{\theta}$ equal to the angle between atomic spins of neighbouring ferromagnetic layers of the spiral structure. For spiral structures considered in the present paper, $\bar{\theta} = \theta$ in the case of BCC lattice and $\bar{\theta} = \frac{1}{2}\theta$ in the case of FCC lattice.

zero. The value of the left boundary $\theta_b$ is defined by the angular dependence of the derivative of the $m_{out} = f(m_{in})$ function at the point $m_{in} = 0$. The exact calculation of this value has serious computational difficulties. Therefore for both Fe and Ni we restricted ourselves to a crude $\theta_b$ estimation. Testing has shown that the variation of $\theta_b$ within reasonable limits does not change the main conclusions of the paper.

Figure 7 shows calculated $E(m)$ curves for various $\theta$. Note that two local minima of the $E(m)$ curve for $\theta = 180°$ correspond to two stable solutions with different $m$. In [11, 14], the question of the existence of the second stable solution was not investigated. Therefore, a conclusion on the extent of this property dependence on physical model cannot be drawn.

We calculated the $m_0(\theta)$ curve within both A and B schemes of self-consistent calculations. As is seen from figure 4 the change of the scheme does not lead to a substantial change of the curve. Therefore, the supposition that the influence of $h_\perp$ reduces to the suppression of the magnetic moment component perpendicular to the chosen direction seems to be correct.

For a state realizing a total energy minimum for a fixed $\theta$, the parallel component of the constraining field is equal to zero. Hence, using values of $h_\perp$ calculated as a function of $\theta$ and also the formula [28]

$$E_0(\beta) = \int_0^\beta h_\perp(\beta) m_0(\beta)\, \mathrm{d}\beta \tag{16}$$

which follows from (15), we can calculate the total energy of these states. The curve thus obtained is shown in figure 5 and is compared with the analogous curve from [11]. On the whole, the curves are in good agreement. In particular, at small $\theta$ our curve is also concave upwards. (This property is important for the picture of spin disordering discussed in [11, 36].) A noticeable difference between the curves takes place for large $\theta$ only.

Figures 6 and 7 show the results of the investigation of the longitudinal static fluc-

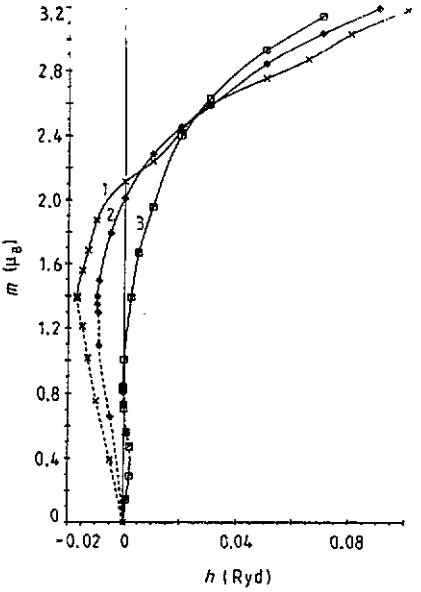


**Figure 6.** The $m(h)$ curves of iron for three values of angle $\theta$: $\theta = 0°$ (curve 1), 90° (curve 2) and 180° (curve 3). The broken parts of curves show unstable states.

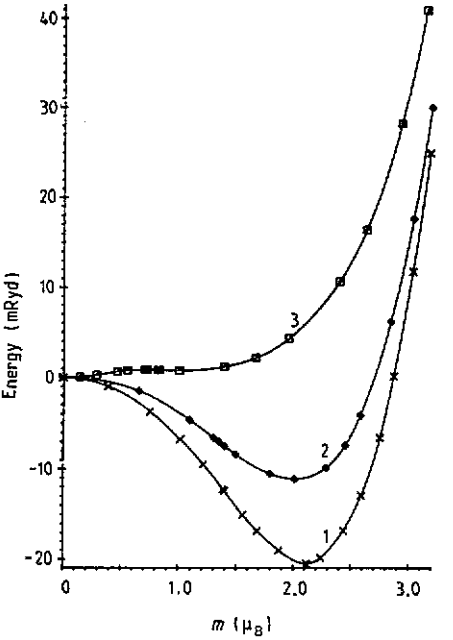


**Figure 7.** The $E(m)$ curves of iron for three values of angle $\theta$: $\theta = 0°$ (curve 1), 90° (curve 2) and 180° (curve 3).

tuations of the local magnetic moment for several angles $\theta$. The calculations of the value of the moment as a function of $h$ (figure 6) were carried out using scheme A. Figure 7 represents corresponding total energy curves evaluated with the formula

$$E(m) = \int_0^m h(m)\,\mathrm{d}m \tag{17}$$

which follows from expression (15). In figure 6 the broken curves show the solutions that are self-consistent but unstable at the relevant values of $h$. In figure 7, these states correspond to the parts of the $E(m)$ curves where the second derivative is negative.

Counting the energies of minima of the functions $E(m)$ off the minimum of the function for $\theta = 0$, we again obtain estimations of some points of the $E_0(\theta)$ curve (figure 5). As is seen from figure 5, the agreement of the results obtained with the help of formulae (16) and (17) is quite good. In the calculations with formula (17) an approximate scheme A was used. Therefore the good agreement of the results may be treated not only as a verification of the accuracy of the calculations but also as a confirmation of the possibility to use scheme A for the study of the longitudinal fluctuations of atomic moments of iron.

Analysis of figures 6 and 7 permits one to draw a number of important conclusions. First, for each $\theta$ there are magnetic moment values that cannot be stabilized by any magnetic field $h$. For $\theta = 0$, these values lie below a point close to 1.39 $\mu_B$. If $\theta = 90°$, the corresponding point is close to 1.37 $\mu_B$. In the case of $\theta = 180°$, the curve $E(m)$ has

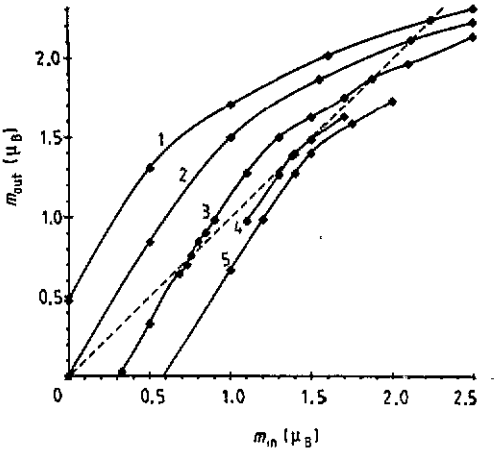


**Figure 8.** The $m_{out} = f(m_{in})$ curve of iron for various values of $h$ and $\theta = 0°$: $h = 10$ (curve 1), 0 (curve 2), $-10$ (curve 3), $-16.8$ (curve 4) and $-20$ (curve 5) mRyd.

two local minima. For the minimum close to 1.01 $\mu_B$ the lower boundary of the magnetic moment values that may be stabilized by a constraining field lies near 0.83 $\mu_B$. For the minimum at $m = 0$ the corresponding values are limited by upper boundary approximately equal to 0.39 $\mu_B$.

The mechanism of the appearance of a critical field $h$ corresponding to the limiting value of local moment is illustrated in figure 8, where the curves $m_{out} = f(m_{in})$ are shown for various $h$. With decrease of $h$ the distance between stable and unstable self-consistent solutions also decreases. For critical $h$ they become equal to each other and a contact of a straight line $m_{out} = m_{in}$ and curve $m_{out} = f(m_{in})$ takes place. For lower $h$, common points of two lines are absent, which corresponds to the absence of self-consistent solutions.

Another important peculiarity consists of the decrease of the depth of the $E(m)$ curve minimum with increase of $\theta$. Coefficients of parabolae describing the $E(m)$ curves near the points of the minima are equal to 0.026, 0.015 and 0.004 for angle $\theta$ equal to 0°, 90° and 180° respectively. These coefficients may be considered as values inverse to 'longitudinal stiffness' of magnetic moments at a given $\theta$. The smaller the coefficient, the larger are the fluctuations of the moment length for the states characterized by this $\theta$. Note that the final value of the longitudinal stiffness of the magnetic moment [2] at a given temperature $T$

$$\tau = (\partial\langle m\rangle/\partial T)^{-1} \tag{18}$$

is also dependent on the position and energy of minima of $E(m)$ for different $\theta$. In (18), $\langle m\rangle$ is a statistically averaged value of local moment length. The important role of parameter $\tau$ for the explanation of temperature properties of itinerant magnets was discussed in detail in [2].

### *3.2. Nickel*

Calculations analogous to those discussed above were carried out for Ni (figures 5 and 9–11). The dependences $m_0(\theta)$ obtained within the framework of different approaches

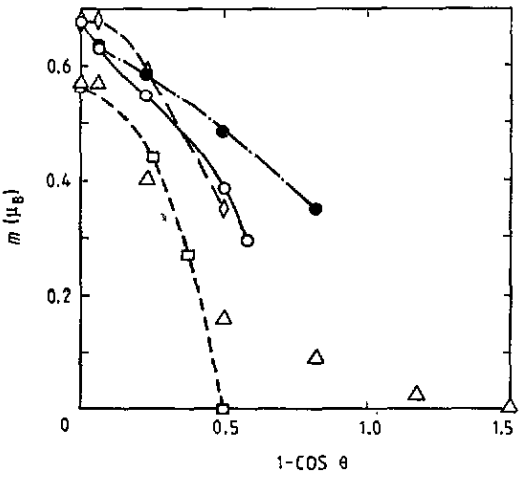


**Figure 9.** The $m_0(\theta)$ functions for Ni. The calculations for spiral structures with $g = (0, 0, 2\pi/a)$: ●, the present calculation, scheme A; ○, the present calculation, scheme B; △, results of [15]; □, results of [17]. The results of our calculations for spiral structures with $\beta = 90°$ and $q$ parallel to the $z$ axis are represented by rhombus (◇). For latter spiral structures schemes A and B are identical. All our calculations have given the second, zero, branch of the $m_0(\theta)$ function. In particular, for spirals with $q = (0, 0, 2\pi/a)$ and calculation scheme B the second branch lies from $\theta_b$, close to 60°, till $\theta = 180°$.

are shown in figure 9. Common features of the results of all calculations are, first, relatively fast, in comparison with iron, decrease of $m_0$ with increase of $\theta$ and, secondly, the zero value of $m_0$ for $\theta = 120°$. Simultaneously, there are substantial differences between calculated dependences. In particular, Haines [17] obtained a faster decrease to zero of $m_0(\theta)$ in comparison with other calculations.

All calculations carried out in the present paper have given $m_0(\theta)$ curves consisting of two branches. Each branch is defined only for a restricted interval of $\theta$ values. One of the branches assumes zero values. The presence of two branches follows identically from the analysis of the $m_{out} = f(m_{in})$ curves calculated for different $\theta$. (The general form of $m_{out} = f(m_{in})$ curves is similar to that shown in figure 2.)

At present we cannot exclude the possibility of the existence of two $m_0(\theta)$ branches for models used in [15, 17]. Indeed, in [15] only the maximal values of self-consistent moment were calculated and the question about a second stable state was not addressed. In [17], the curves $m_{out} = f(m_{in})$ were considered but for a very rare grid of angle $\theta$.

Another important conclusion following from the analysis of figure 9 is an essential difference of the $m_0(\theta)$ curves obtained within different schemes of self-consistent calculations. The allowance for the perpendicular component $h_\perp$ of the constraining field leads, in the case of nickel, to the substantially faster decrease of $m_0$ with $\theta$ increase. The previous investigations [14, 15] permit one to explain this in terms of the different influences of the explicit allowance for $h_\perp$ in the cases of Fe and Ni. Indeed, the value of $h_\perp$ enters into the non-diagonal blocks of secular matrix (11) and influences, first of all, the extent of hybridization of opposite spin states. As was discussed in [14, 15], the influence of interspin hybridization upon the value of the local moment in iron is substantially weaker than in nickel. This property is directly connected with the peculiarities of electronic structure of Fe and Ni [15].

In figures 10 and 11, the curves $m(h)$ and $E(m)$ are represented, which characterize the longitudinal fluctuations of magnetic moments. All calculations for Ni were carried out with the use of scheme B. As in the case of iron, there are magnetic configurations that cannot be stabilized by any 'external' field. In particular, for $\theta = 0$ the minimal possible value of $m$ is close to 0.47 $\mu_B$. The other property of the longitudinal fluctuations of iron also remains true in the case of Ni: with increase of $\theta$ the depth of the $E(m)$ minimum at non-zero value of $m$ becomes less. That is, the longitudinal stiffness at a

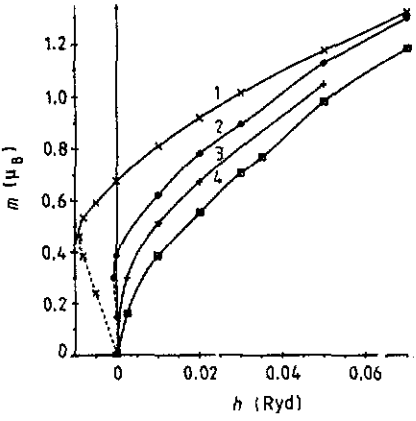


**Figure 10.** The $m(h)$ curves of nickel for angles $\theta = 0°$ (curve 1), 60° (curve 2), 90° (curve 3) and 120° (curve 4). The broken parts of curves show unstable states.

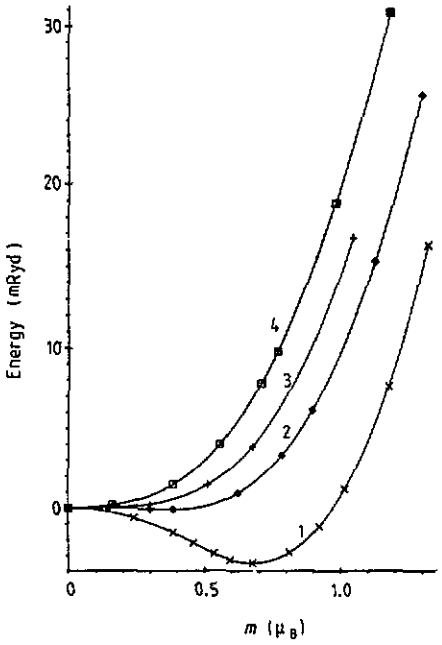


**Figure 11.** The $E(m)$ curves of nickel for angles $\theta = 0°$ (curve 1), 60° (curve 2), 90° (curve 3) and 120° (curve 4).

fixed $\theta$ decreases with increase of $\theta$. For a critical value of $\theta$ where the stable solution at non-zero $m$ disappears, longitudinal stiffness becomes practically zero. For the stable state with zero $m_0$, in contrast, the longitudinal stiffness at a fixed $\theta$ increases with increase of $\theta$ (figure 11).

## 4. Simple scheme of statistical averaging

The information about excited states of Fe and Ni discussed in the previous section can be used within the framework of different schemes of statistical averaging aimed at the calculation of temperature dependences of electronic properties. Consideration of various schemes of averaging, comparison of the results thus obtained with experimental data, and choice of the most reliable method present a serious problem. In this paper, we restrict ourselves to the consideration of a simple averaging scheme corresponding to the paramagnetic state. The results of calculations are compared with the respective results of Hubbard [4, 37, 38].

As in [4, 37, 38], let us focus on the consideration of one atom. We suppose that the number of magnetic configurations for which the average angle between the spin of this atom and the spins of neighbouring atoms is equal to $\theta$ is proportional to $g(\theta)$. To model two opposite limits of short-range magnetic order (SRMO) we shall consider two different forms of $g(\theta)$.

Let symbol $k$ number the nearest neighbours of the atom considered and $\theta_k$ be the angle between the central atom and the $k$th nearest neighbour. In the limit of very strong

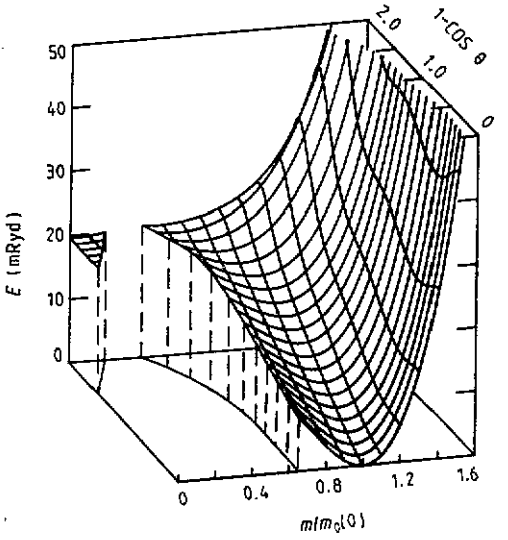


**Figure 12.** Total energy of stable states in the case of iron. The projection of the total energy surface on the $\theta$–$m$ plane shows the integration area in formula (19).

ferromagnetic SRMO all $\theta_k$ are approximately equal to one another and, as a result, the average angle

$$\theta = \frac{1}{n}\sum_k \theta_k$$

($n$ is the number of nearest neighbours) is approximately equal to any of the $\theta_k$. Hence to estimate $g(\theta)$ we can consider the central atom and any one of its neighbours. For two spins that can assume arbitrary relative directions, the number of configurations with given interspin angle $\theta$ is proportional to sin $\theta$. Therefore the first form of $g(\theta)$ we shall use is $g_1(\theta) = \sin\theta$.

If we suppose that SRMO is negligible, the angles $\theta_k$ should be considered as independent values. Then [39] the dispersion of $g(\theta)$ distribution is $n$ time smaller than for every $\theta_k$ value. To model this property we shall consider the second form of $g(\theta)$, $g_2(\theta) = \delta(\theta - \pi/2)$, which corresponds to an infinitely narrow distribution. (This distribution is correct in the limit of $n$ tending to infinity.)

The partition sum corresponding to the states of the atom considered will be assumed to be proportional to the integral

$$\int_0^\pi d\theta\, g(\theta) \int_{(m_\theta)} \mathrm{d}m\, f(m) \exp[-E(\theta, m)/T] \tag{19}$$

where $(m_\theta)$ denotes integration over values of $m$ stable for a given $\theta$. In the case of Fe the integration area may be seen in figure 12. (We restrict the integration to stable states because only states corresponding to the minimum of total energy are considered, within the density-functional approach, as those which may be really occupied by the system.)

Depending on the adopted scheme of averaging the function $f(m)$ in (19) may assume two different forms [38]:

$$f_1(m) = 1 \tag{20a}$$

or

$$f_2(m) = m^2. \tag{20b}$$

The choice of $f(m)$ in the form (20$b$) means that all states enter into the partition sum

on an equal footing and their contribution is defined by the energy of the corresponding states only. The appearance in this case of the multiplier $m^2$ is connected with the Jacobian of the spherical coordinate system. The choice of $f(m)$ in the form (20*a*) corresponds to the supposition that at first the averaging over $m$ is carried out for each $\theta$ and then the values obtained are averaged over $\theta$. The latter scheme of averaging seems to be closer to the approach used in [5] within the framework of the KKR-CPA method, where the excited states of the system are assumed to be characterized identically by the unit vectors showing the directions of atomic magnetic moments. The lengths of magnetic moments do not influence the contribution of states to the partition sum [5].

As we consider the paramagnetic state, the magnitude of average magnetization does not enter into (19).

Changing the order of integration in (19) we obtain

$$\int_0^\infty \mathrm{d}m\, f_i(m) \int_{(\theta_m)} \mathrm{d}\theta\, g_j(\theta) \exp[-E(\theta,m)/T] = \int_0^\infty \mathrm{d}m\, p_{ij}(m). \tag{21}$$

Here $(\theta_m)$ denotes the integration over angles $\theta$ for which the given value of $m$ is stable.

The probability density for the local magnetic moment length will be estimated using the formula

$$p(m) = P(m) \Big/ \int_0^\infty \mathrm{d}m\, P(m). \tag{22}$$

Note that a consistent statistical-mechanics model must be self-consistent as regards the input and output extent of the SRMO. Simple calculations based on formula (19) do not satisfy this condition. However they permit one to estimate the limits of the dependence of $P(m)$ distribution on the extent of SRMO.

To calculate integrals (21) an interpolation of $E(\theta,m)$ was carried out. First, the energy of the minimum of $E(m)$ (see e.g. figure 5) was interpolated as a function of $\theta$. Then the $E(m)$ curves corresponding to various $\theta$ (figures 7 and 11) were interpolated, for a fixed $\theta$, with a fourth-order polynomial of $m - m_0(\theta)$. Calculated coefficients at second, third and fourth degrees were also interpolated as the function of $\theta$. The interpolation thus obtained allowed us to restore the $E(m)$ curve for any $\theta$. In the case of Fe, the calculated $E(\theta,m)$ surface corresponding to the stable states is shown in figure 12. Note that in the case of FCC structure the calculated spiral configurations cover the interval of $\theta$ from 0 to 120°. Therefore, in consideration of Ni an extrapolation was used for angles 120–180°.

In figure 13, the curves $p(m)$ calculated for iron are shown. The curves $p_{1j}(m)$ and $p_{2j}(m)$ appear to be rather close to each other for both values of $j$. Naturally, curve $p_{2j}(m)$ is somewhat shifted to larger values of $m$ relative to $p_{1j}(m)$ because of the additional multiplier $m^2$ in (21). The closeness of the curves $p_{1j}(m)$ and $p_{2j}(m)$ means that the most probable values of magnetic moment are distributed within a rather narrow interval. Hence, one can draw a conclusion that in iron there is a fairly well defined local moment. The states connected with the zero branch of the $m_0(\theta)$ function do not make a marked contribution to $p(m)$. A sharp increase of $p(m)$ near $m = 1.39\mu_B$ is a consequence of the fact that for a wide interval of $\theta$ the boundary between stable and unstable states passes near this value (figure 12).

The comparison (figure 13) shows that in the case of iron the dependence of $p(m)$ distribution on the form of function $g(\theta)$ is rather weak. The replacement of $g_1(\theta)$ by

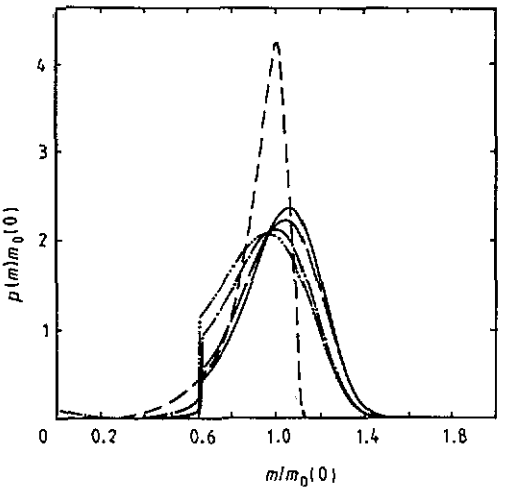


**Figure 13.** Probability density of magnetic moment length in the case of iron: – – –, curve of [4, 38] calculated with $f_2(m) = m^2$ for $T = 1.09T_C$. Present calculations: –·–·–, $p_{11}(m)$; –··–··–, $p_{12}(m)$; ———, $p_{21}(m)$; — —, $p_{22}(m)$. In our calculations the experimental value of $T_C$ = 1043 K has been used.

$g_2(\theta)$ does not influence substantially the general form, the position of the maximum and even the quantitative characteristics of $p(m)$. This weak dependence of the distribution of the amplitude of magnetic moment on the extent of the SRMO is one more argument for the presence of well defined local moments in iron.

Figure 13 also contains the curve $p_{21}(m)$ from [4, 38]. (We use the notation $p_{21}$ for the curve of [4, 38] because in the formula for the partition sum [4, 38] the integral over the amplitude of random fields contains a multiplier analogous to $f_2$ and the integral over angular variable includes a factor analogous to $q_1$.) Comparison of $p_{21}(m)$ with our corresponding curves $p_{2j}(m)$ shows that they are qualitatively similar: all of them have a sharp maximum near the value of the ground-state magnetic moment and are quite narrow. However, there are noticeable quantitative differences. Our distribution appears to be more diffuse. We associate this difference with two factors. The first is the consideration, in [4], of d electrons only. As a result, the local magnetic moment could not be more than 2.5 $\mu_B$ for any excited state. The second factor is connected with the difficulty of taking into account the angular dependence of $E(m)$ minimum depth within the framework of the single-site approximation used in [4].

Curves $p(m)$ in the case of Ni are plotted in figure 14. Calculations have shown that distributions $p_{2j}(m)$ keep, on the whole, the form of the corresponding curves of Fe (figure 13) although they are substantially more diffuse. However, the form of $p_{1j}(m)$ curves changes drastically in comparison with the corresponding curves of iron. In particular, both curves $p_{1j}(m)$ have a maximum at $m = 0$. The replacement of $g_1(\theta)$ by $g_2(\theta)$ also leads, in the case of Ni (figure 14), to a substantial change of $p(m)$ distribution. This sensitivity of $p_{ij}(m)$ function to the values of parameters $i$ and $j$ shows that we cannot treat Ni as a metal with well defined local atomic moments. It is also important that the choice of averaging scheme is crucial in the cases of Ni and can drastically change the results of calculations.

Comparison, in figure 14, of our curves with those of Hubbard [37, 38] shows that both calculations give an analogous character of the change of distribution $p(m)$ on transition from the case $g = g_1$ to the case $g = g_2$. However, the curves calculated with the same $g(\theta)$ but within two different approaches differ considerably. In particular, Hubbard's distribution $p_{21}(m)$ appeared to be more narrow than his curve $p_{21}(m)$ in the case of Fe. On the contrary, our curve $p_{2j}(m)$ is substantially more diffuse than our

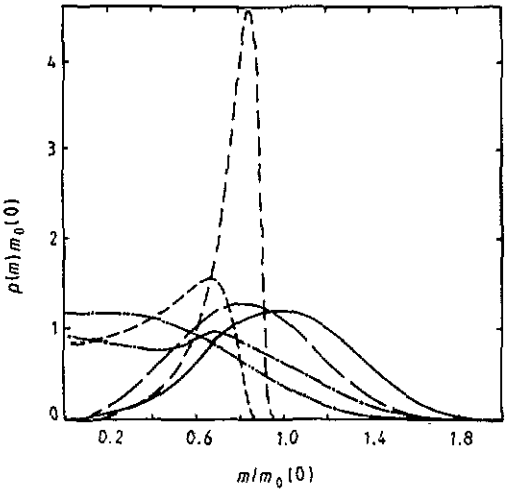


**Figure 14.** Probability density of magnetic moment length in the case of nickel: – – –, curve of [38] calculated with $f_1(m) = 1$ for $T = 1.38T_C$; — — —, curve of [37, 38] calculated with $f_2(m) = m^2$ for $T = 1.23T_C$. Present calculations: –·–·–, $p_{11}(m)$; ·····, $p_{12}(m)$; ——, $p_{21}(m)$; ————, $p_{22}(m)$. In our calculations the experimental value of $T_C = 631$ K has been used.

corresponding curve in the case of Fe. To some extent the distinction of curves may be explained using the same arguments as in the case of Fe. First, the allowance for the d electrons only [37, 38] reduces the region of possible $m$ values. In particular, any excited state has local magnetic moment smaller than or equal to $m_0(0)$. The second point is connected with the difficulty of taking into account the angular dependence of longitudinal stiffness within the calculational scheme of [37, 38]. However, these arguments seem to be insufficient to explain such small 'smearing' of the curve $p_{21}(m)$ of [37, 38]. We cannot point out the peculiarities of the physical model of [37, 38] that lead to such a narrow $p_{21}(m)$ distribution, especially taking into account that the $p_{11}(m)$ curve of [37, 38] gives almost uniform distribution of moment lengths in a wide interval lying on the left from maximum of $p_{21}(m)$.

Figure 15 shows the temperature dependence of average length, $\langle m \rangle$, of local magnetic moments, which is calculated using distributions (22). The values of $\langle m \rangle$ differ for different distributions. In accordance with the previous discussion, the relative difference of these values in the case of Fe is much smaller than in the case of Ni. The temperature variation of average local moment of Fe is also weak, for all $p_{ij}(m)$, and does not exceed a few hundredth of a Bohr magneton. In the case of Ni, the situation is substantially different: for $p_{11}(m)$ and $p_{21}(m)$ distributions the scale of temperature variation of average magnetic moment is comparable with its value at $T_C$; for $p_{12}(m)$ and $p_{22}(m)$ distributions the variation is weaker but nevertheless exceeds 10%.

The temperature dependence of $\langle m \rangle$ was also estimated neglecting the longitudinal fluctuations of moments, that is assuming that the only magnetic configuration corresponds to each set of atomic moment directions [5]. The formula used was

$$\langle m \rangle = \frac{\int_0^\pi d\theta\, m_0(\theta)\, g(\theta) \exp[-E_0(\theta)/T]}{\int_0^\pi d\theta\, g(\theta) \exp[-E_0(\theta)/T]} \qquad (23)$$

If we compare the results obtained with the same $g(\theta)$, the neglect of amplitude fluctuations leads to smaller values of $\langle m \rangle$ (figure 15(*c*)) than in the case of the use of distributions (22) (figures 15(*a*) and (*b*)). However, in the case of Fe this change of average length of moments is much less. These results correlate with the results of the calculations within the KKR-CPA method [9], which also gave the paramagnetic local moment of Fe to be close to the ground-state value.

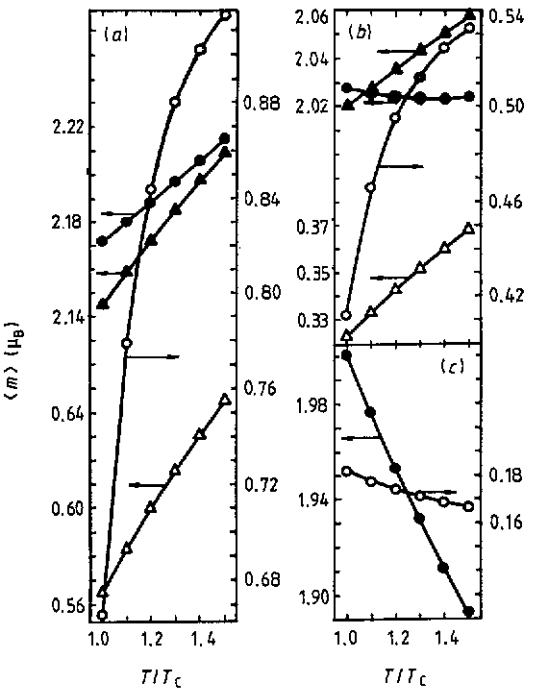


**Figure 15.** Temperature dependence of average magnetic moment length calculated with the use of (*a*) $f = f_2(m)$, and (*b*) $f = f_1(m)$ functions and (*c*) of formula (23): ●, Fe, $g = g_1(\theta)$; ▲, Fe, $g = g_2(\theta)$; ○, Ni, $g = g_1(\theta)$; △, Ni, $g = g_2(\theta)$. In the case of neglect of amplitude fluctuations (formula (23)) the use of $g = g_2(\theta)$ leads to a value of $\langle m \rangle$ independent of temperature: 2.034 $\mu_B$ for Fe and 0.0 $\mu_B$ for Ni.

Most calculations allowing for longitudinal fluctuations within the Hubbard Hamiltonian approach (see e.g. [2]) give an increase of $\langle m \rangle$ with heating. In our calculations, the use of the function $f_2(m) = m^2$ to make an allowance for amplitude fluctuations (figure 15(*a*)) also leads, in all cases, to the increase of $\langle m \rangle$. However, the use of the function $f_1(m) = 1$ (figure 15(*b*)) results, for the $p_{11}(m)$ distribution of Fe, in a very weak and non-monotonic dependence of $\langle m \rangle$. Finally, neglect of amplitude fluctuations (figure 15(*c*)) gives, in all cases, the constancy or decrease of $\langle m \rangle$ with increase of temperature. Thus different approaches to the consideration of amplitude fluctuations give essentially different characters for the temperature dependence of $\langle m \rangle$. The comparisons carried out show that due account for amplitude fluctuations is the important point of a consistent statistical-mechanics model.

Note that, as we are interested in temperature behaviour of physical properties, the 'smearing' of the Fermi step with increase of temperature is to be taken into account in the course of band-structure calculations. However, our estimations have shown that this mechanism has a weak influence on the form of the $p(m)$ distribution. In particular, for both Fe and Ni the use of the Fermi function corresponding to the Curie temperature leads to a change of the values of $m_0(\theta)$ functions (figures 4 and 9) which, for the most part, does not exceed a few per cent.

## 5. Conclusions

A calculation scheme is realized that permits one to investigate both transverse and longitudinal fluctuations of local magnetic moments and is based on the use of a band-structure calculation method for the study of excited magnetic states. Some comparisons are made illustrating the role of allowance for longitudinal fluctuations as well as the role of detailed study of electronic characteristics of excited magnetic configurations.

Evidently, the question about the necessity and methods of taking static amplitude fluctuations of magnetic moments into account demands further considerable efforts (see e.g. discussion in [5, 19]). A reliable answer to this question may be obtained only within the framework of a more general theory, which makes allowance for dynamic effects. This problem is very complicated and is not discussed in the present paper.

## Acknowledgment

The authors would like to thank P G Guletskii for consultations in programming.

## References

[1] Moruzzi V L, Janak J F and Williams A R 1978 *Calculated Electronic Properties in Metals* (New York: Pergamon)
[2] Moriya T 1985 *Spin Fluctuations in Itinerant Electron Magnetism* (Berlin: Springer)
[3] Korenman V, Murray J L and Prange R E 1977 *Phys. Rev.* B **16** 4032
[4] Hubbard J 1979 *Phys. Rev.* B **20** 4584
[5] Gyorffy B L, Pindor A J, Staunton J, Stocks G M and Winter H 1985 *J. Phys. F: Met. Phys.* **15** 1337
[6] You M V and Heine V 1982 *J. Phys. F: Met. Phys.* **12** 177
[7] Hasegawa H 1979 *J. Phys. Soc. Japan* **46** 1504
[8] Oguchi T, Terakura K and Hamada N 1983 *J. Phys. F: Met. Phys.* **13** 145
[9] Pindor A J, Staunton J, Stocks G M and Winter H 1983 *J. Phys. F: Met. Phys.* **13** 979
[10] Holden A I and You M V 1982 *J. Phys. F: Met. Phys.* **12** 195
[11] Luchini M U and Heine V 1989 *J. Phys.: Condens. Matter* **1** 8961
[12] Haines E M, Heine V and Ziegler A 1986 *J. Phys. F: Met. Phys.* **16** 1343
[13] Sandratskii L M and Guletskii P G 1988 *Fiz. Met. Metalloved. (USSR)* **65** 234
[14] Sandratskii L M and Guletskii P G 1989 *J. Magn. Magn. Mater.* **79** 306
[15] Sandratskii L M and Guletskii P G 1989 *Phys. Status Solidi* b **154** 623
[16] Guletskii P G, Knyazev Yu V, Kirillova M M and Sandratskii L M 1989 *Fiz. Met. Metalloved.* **67** 279
[17] Haines E M 1989 *Solid State Commun.* **69** 561
[18] Samson J H 1989. *J. Phys.: Condens. Matter* **1** 6717
[19] Capellmann H 1987 *Metallic Magnetism* ed H Capellmann (Berlin: Springer) p 1
[20] Sandratskii L M 1985 *Fiz. Met. Metalloved.* **59** 7
[21] Sandratskii L M and Guletskii P G 1986 *J. Phys. F: Met. Phys.* **16** 143
[22] Sandratskii L M 1986 *Phys. Status Solidi* b **135** 167
[23] Kübler J, Höck K-H, Sticht J and Williams A R 1988 *J. Phys. F: Met. Phys.* **18** 469
[24] Sticht J, Höck K-H and Kübler J 1989 *J. Phys.: Condens. Matter* **1** 8155
[25] Slater J C and Koster G F 1954 *Phys. Rev.* **94** 1498
[26] Papaconstantopoulos D A 1986 *Handbook of the Band Structure of Elemental Solids* (New York: Plenum)
[27] Sandratskii L M 1990 *Solid State Commun.* **75** 527
[28] Dederichs P H, Bluger S, Zeller R and Akai H 1984 *Phys. Rev. Lett.* **53** 2512
[29] Edwards D M 1984 *J. Magn. Magn. Mater.* **45** 151
[30] Small L M and Heine V 1984 *J. Phys. F: Met. Phys.* **14** 3041
[31] Schwarz K and Mohn P 1984 *J. Phys. F: Met. Phys.* **14** L129
[32] Moruzzi V L, Marcus P M, Schwarz K and Mohn P 1986 *Phys. Rev.* **34** 1784
[33] Moruzzi V L 1986 *Phys. Rev. Lett.* **57** 2211
[34] Moruzzi V L, Marcus P M and Kübler J 1989 *Phys. Rev.* B **39** 6957
[35] Luchini M U and Nex C M M 1990 *J. Phys.: Condens. Matter* **2** 3497
[36] Heine V and Joynt R 1988 *Europhys. Lett.* **5** 81
[37] Hubbard J 1981 *Phys. Rev.* B **23** 5974
[38] Hubbard J 1981 *Electron Correlation and Magnetism in Narrow-Band Systems* ed T Moriya (Berlin: Springer) p 29
[39] Korn G A and Korn T M 1968 *Mathematical Handbook for Scientists and Engineers* (New York: McGraw-Hill)